JOURNAL OF MATERIALS SCIENCE 18 (1983) 103–108

Microstructural effects of fatigue crack growth in a two-phase steel

T. ISHIHARA
Ishikawajima-Harima Heavy Industries Co, Ltd, Aero-engine and Space Operations, 3-5 Mukodai-cho, Tanashi-shi, Tokyo, Japan

A study has been made of the influence of microstructure on fatigue crack growth in a two-phase steel, in which islands of ferritic phase are encapsulated by the martensitic phase in association with cleavage cracking of ferrite grains. High mean stress has a significant effect on the crack propagation and on the high strength ratio (hardness) between martensite and ferrite.

1. Introduction

The dependence of fatigue crack-propagation rate, da/dN, on alternating stress-intensity factor, $\Delta K = K_{max} - K_{min}$, is generally expressed by the relationship [1, 2]:

$$da/dN = C\Delta K^m$$

where C and m are constants, a is the crack length and N the number of fatigue cycles. However, it is believed that other factors, such as microstructure, temperature, mean stress and material properties, can markedly influence fatigue crack growth [3, 4]. The effects of mean stress are particularly important. Although many investigations have been made into such effects, they have been exhaustive. Ritchie and Knott [5], Richards and Lindley [6], Suzuki and McEvily [7] and Ishihara [8] have suggested that the general effect of mean stress on the rates of fatigue crack propagation may be due to modes of "static" or monotonic fracture which can occur in addition to characteristic striation growth. Segments of fracture are also thought to be promoted by an increase in mean stress, and to lead to accelerated fatigue crack-growth rates. Therefore, certain dual-phase steels can be heat-treated in such a way as to develop two-phase microstructure with special shapes. The strength, toughness, ductility, etc., of these structures have been studied and the behaviour related to microstructural properties. However, crack propagation leading to fatigue crack growth has not been explored in any detail, and because of the interesting morphological relationships which can develop between the phases, it appeared worthwhile to explore the fatigue crack propagation in a two-phase microstructure under a high mean stress where the influence of microstructure is known to be of importance. Through appropriate heat-treatment procedures, unique types of microstructure were developed in a low carbon steel, which consisted of islands of ferrite within a continuous martensite network. The characteristic behaviour of crack propagation in a two-phase microstructure under a high mean stress might be expected to show a strong dependence on the strength (hardness) ratio of the constituent microstructures. Therefore, in the present paper, attention is focused on crack growth in a two-phase microstructure where the strength ratio of the microstructure is successively lowered by tempering the ferrite–martensitic steel at various temperatures. The effect of metallurgical parameters on the micro-cracking process is viewed with special interest. It has been shown that the mechanical properties of these microstructures were associated with the effects of interaction between these two phases rather than the individual properties of martensite and ferrite. It is recognized that fracture occurs in a brittle manner in this microstructure, accompanying cleavage cracking of the ferrite grains. This unusual cleavage cracking behaviour of the ferrite grain may be reasonably explained by the changes of internal stress associated with phase-strength transformation of the martensite and also with the plastic constraint produced by the martensite during the

0022–2461/83/010103–06$03.22/0

TABLE I Chemical composition (wt %)

	C	Si	Mn	P	S	Cu	Ni	Cr
S25C	0.22	0.20	0.43	0.019	0.010	0.01	0.01	0.01

loading process. However, questions arise as to how a high mean stress at a high strength ratio influences crack propagation and also what effects low-strength ratio has on these properties.

2. Experimental procedure

A low carbon steel, the chemical composition of which is shown in Table I, was chosen for the investigation. The specimens for fatigue crack-growth tests were of the tension–tension type with a total height of 157 mm; the effective width was 39 mm, and the thickness was 6 mm as shown in Fig. 1 [9].

In order to develop the desired two-phase microstructure, the heat-treatment procedures given in Table II were followed. Quantitative metallographic techniques were employed to determine the ferrite grain size, the volume fraction of martensite, the size of the martensitic structure, and the degree of connectivity of the martensitic structure.

This treatment leads to the type of microstructure shown in Fig. 2. The martensitic phase is continuous, with the ferritic phase isolated within the martensitic phase.

Quantitative metallographic techniques were employed to determine the ferrite grain size, the volume fraction of martensite, the size of the martensitic structure, and the degree of connectivity of the martensitic structure.

The continuous martensitic phase which encapsulates a ferritic structure is called a "continuous-martensitic network" (abbreviated R0). The connectivity of the martensitic structure is defined by the parameter $\bar{O}$, where $\bar{O} = N_g/N_g + N_b$, and N_g is the average number of intersections made with the boundaries of the martensitic structure per unit length (mm^{-1}), and N_b is the average number of intersections with the grain boundaries of the ferrite per unit length (excluding the length shared by the martensitic structure, in mm^{-2}). Four types of fatigue test pieces having different martensitic hardness without changing the ferritic grain size, the connectivity and the volume fraction of martensite, were made. In order to change only the martensitic hardness, R0 material is tempered at three different temperatures: 473, 673 and 873 K (abbreviated R2, R4 and R6, respectively). Table III shows the quantitative evaluation of R0 by the line counting method using such microstructural parameters as volume fraction of martensite grain size and the micro-Vikers martensitic hardness of each material (measured using a Vikers microhardness tester, 20 g load and average of 100 points).

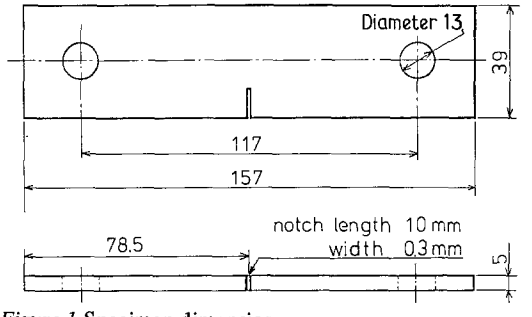

Figure 1 Specimen dimensions.

Fig. 3 shows a comparison of the martensitic hardness for R0, R2, R4 and R6, together with their mechanical properties.

The fatigue tests were carried out in hydraulic testing machine under following conditions: mean stress, σ_m, 39, 126 MPa; stress range, $\Delta\sigma$, 49 MPa with sinusoidal waves in laboratory air; cyclic frequency, 30 Hz. 20 electron micrographs were taken every 10^{-2} mm at the centre of the crack surface in the direction of cracking.

3. Results and discussion

The results of the fatigue crack propagation tests

TABLE II Heat-treatments

Step 1	Homogenize at 1478 K for 1 h; furnace-cool to room temperature.
Step 2	Reheat to 1423 K for 3 h to obtain the desired austenite grain size; furnace-cool to room temperature.
Step 3	Reheat to 1030 K and hold for 40 min in the salt bath; air-cool. Repeat this process twice. The purpose of this multiple heat-treatment is to revert the pearlite to austenite and to develop a continuous austenite network along the ferrite boundary without developing a coarsened ferrite structure.
Step 4	Reheat to 1060 K, in the salt bath, quench in ice water to transform the newly formed austenite to martensite.

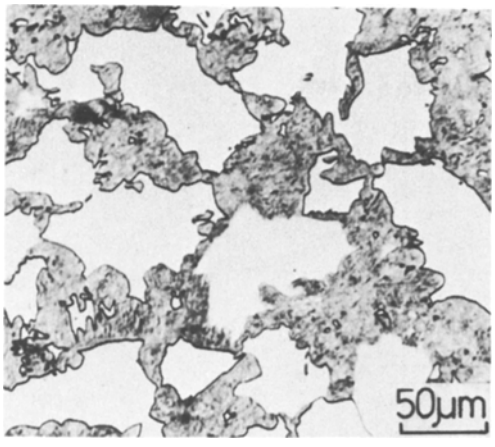

Figure 2 Typical microstructure of a two-phase steel.

are plotted in Figs. 5 to 9 as crack growth rate, da/dN, against ΔK. The fatigue crack-growth behaviour has been studied for several mean stress values; the marterials used were R0 to R6 which have stress–strain curves as shown in Fig. 4.

The following equation was used to calculate the stress intensity range, ΔK $(= K_{max} - K_{min})$ [10]:

$$\Delta K = \Delta\sigma(\pi a)^{1/2} F\left(\frac{a}{W}\right)$$

where

$$F\ \frac{a}{W} = \left(\frac{2W}{\pi a}\right)^{1/2} \cdot \tan\frac{\pi a}{2W} \times \frac{0.75 + 2.02(a/W) + 0.37\{1 - \sin(\pi a/2W)\}^3}{\cos(\pi a/2W)},$$

a is the crack length, and W the width of test piece. Fig. 5 shows fatigue crack propagation curves when the mean stress was varied from 21 to 126 MPa. Two mean stress values were selected from Fig. 5: $\sigma_m = 39$ Mpa which is rather low, and $\sigma_m = 126$ MPa which is very high. The crack propagation rate for various strength ratios at these mean stress values is shown in Figs. 6 to 9. When the mean stress increases, the crack propagation behaviour at $\sigma_m = 39$ and 126 MPa is markedly different.

TABLE III Metallurgical properties

	Martensitic structure		Ferritic structure		$\bar{O}$ (%)
	volume fraction (%)	Hardness (H_V 20 g)	Grain size (μm)	Hardness (H_V 20 g)	
R	50.8	836	73	240	98.5

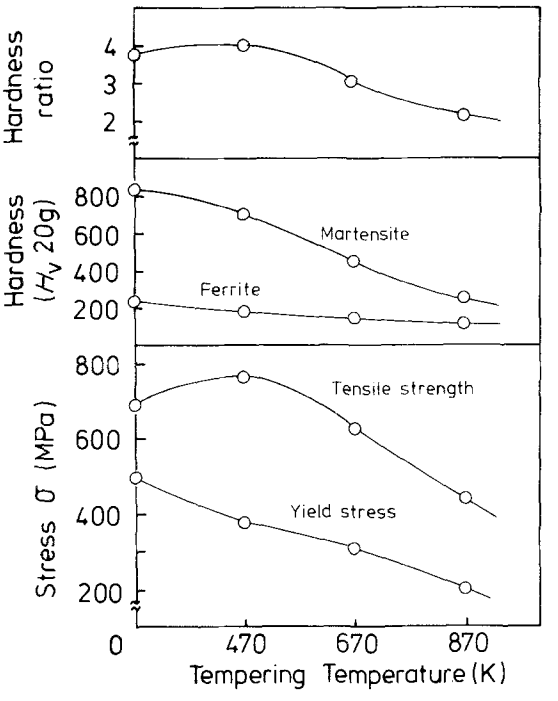

Figure 3 The relationship between mechanical hardness properties and tempering temperature.

Fig. 6 shows the crack propagation at a high strength ratio and mean stresses of $\sigma_m = 26$ to 126 MPa. It can be seen that at 126 MPa the crack propagation does not depend on mean stress. On the other hand, scanning electron microscopy of the fracture surfaces of material R0, $\eta = 3.9$ at $\sigma_m = 126$ MPa, revealed the results shown in Fig. 10. Large amounts of cleavage were observed (Fig. 10) as the mean stress markedly increased to 126 MPa, thus accelerating the overall fatigue crack propagation. However, when the strength ratio, η, was decreased ($\eta = 2873$ K

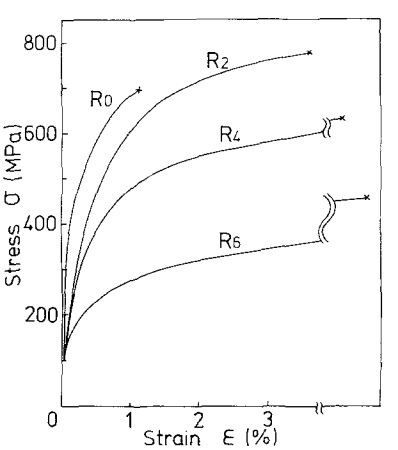

Figure 4 Stress–strain curves.

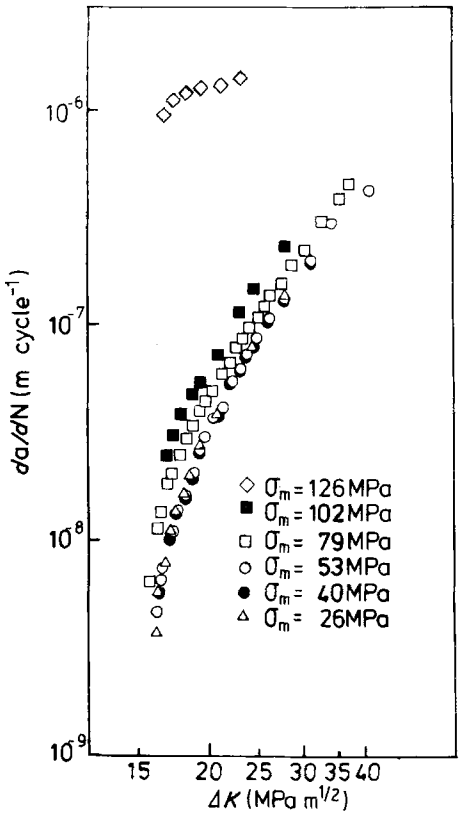

Figure 5 The relationship between crack propagation rate and stress intensity factor for R0, $\eta = 3.9$.

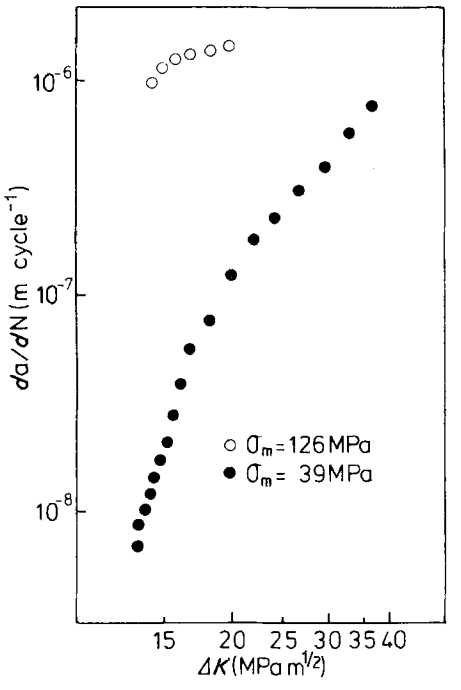

Figure 6 The relationship between crack propagation rate and stress intensity factor for R0, $\eta = 3.9$.

tempering), the crack propagation rates at mean stresses of 39 and 126 MPa, are similar. It is important to know the size of the cyclic plastic zone R_{yc}, and the plastic constraint, χ, for martensite in order to determine crack propagation behaviour under these two-phase microstructures.

It is also interesting to evaluate crack propagation under these two-phase microstructures. It is known that the following equation is effective in determining the internal stress at the matrix by plastic constraint [11]:

$$\chi = 1 + \frac{(2\nu - 1)}{6(\nu - 1)} \left[1 - (\gamma_2/\gamma_1)^{-2} \left\{\frac{M\sigma_y}{F\sigma_y} - 1\right\}\right] \quad (1)$$

where χ is the plastic constraint factor, ν Poisson's ratio; $M\sigma_y$ the yield stress of martensite; $F\sigma_y$ the yield stress of ferrite; γ_1 the radius of martensite; and γ_2 the external radius of ferrite. Equation 1 can be approximated as

$$\chi \simeq (1 + C)(M\sigma_y/F\sigma_y - 1)$$

$$\simeq f(M\sigma_y/F\sigma_y) \propto \frac{M(H_V)}{F(H_V)} = \rho_{H_V}$$

Therefore, it is possible to determine χ for the crack propagation behaviour from the plastic zone size and variation of strength ratio, η, if the martensite volume fraction, grain size and connectivity are almost equal [12]. Table IV shows the calculated cyclic plastic zone size; the plastic zone size at a mean stress of 79 MPa almost equals the grain size.

Judging from Equation 1, χ will be larger in the case of $\eta = 4$ than $\eta = 2$. Therefore, it is natural that cleavage facets occur easily under the conditions in which grain size is smaller than that of the plastic zone size and χ show a large value. Of course many cleavage facets are observed through scanning electron microscopy, as seen in Fig. 10. The cyclic-plastic zone size is smaller than the grain size at $\eta \sim 2$, and as the increase in internal stress is low and χ is rather low at $\eta \sim 2$, so it will become impossible for cleavage facets to occur. For this reason, the crack propagation rate will be slower. Even if the shape of a continuous-martensite network remains in the structure, fast crack propagation is not expected by means of cleavage facets under $\eta \sim 2$ if the mean stress is high. It is almost impossible to see cleavage facets on the fracture. Therefore, the crack growth rate, da/dN, at $\sigma_m = 126$ MPa becomes equal to that at $\sigma_m = 39$ MPa. The following points should be

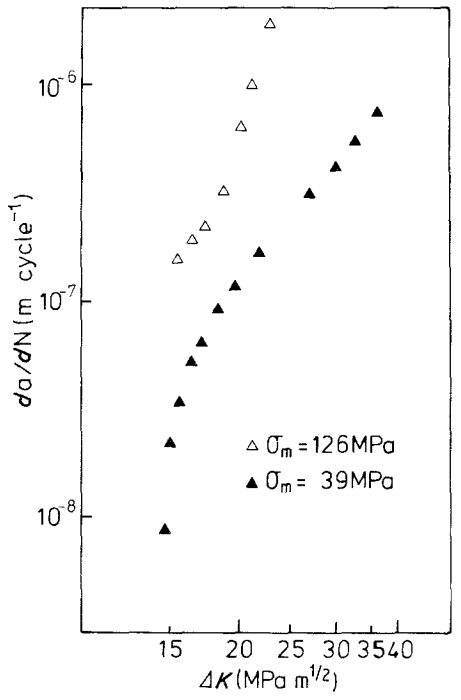

Figure 7 The relationship between crack propagation rate and stress intensity factor for R2, $\eta = 4.0$.

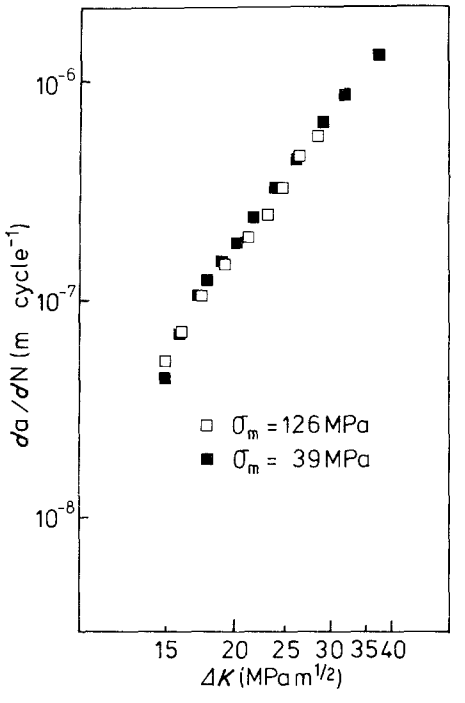

Figure 9 The relationship between crack propagation rate and stress intensity factor for R6, $\eta = 2.0$.

made when comparing our work with that of Suzuki and McEvily [7]. Both works adopted a low carbon steel to observe cleavage cracking of ferrite (grain). Therefore, the heat-treatment is apparently similar but each temperature and holding time is different. Suzuki and McEvily's metallurgical properties differ from those in the present work; the volume fraction, hardness of martensite and the grain size of ferrite used were much lower than those in this work. It is very difficult to compare the present results with those of Suzuki and McEvily because these factors are very effective in fatigue crack propagation. In addition, the hardness of the second phase (= martensite) is changed in the present work in order to investigate

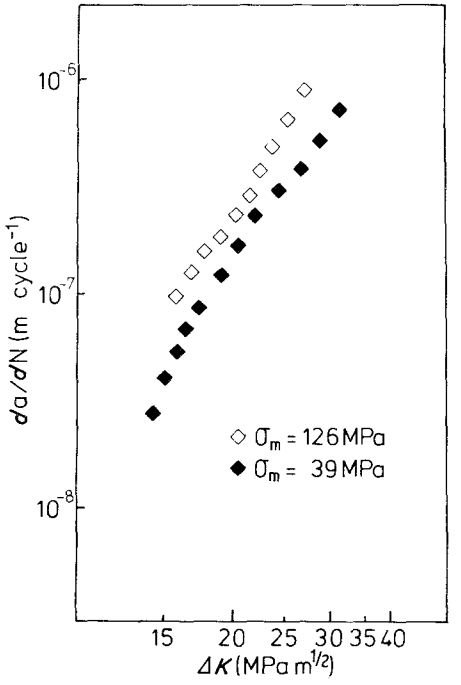

Figure 8 The relationship between crack propagation rate and stress intensity factor for R4, $\eta = 3.0$.

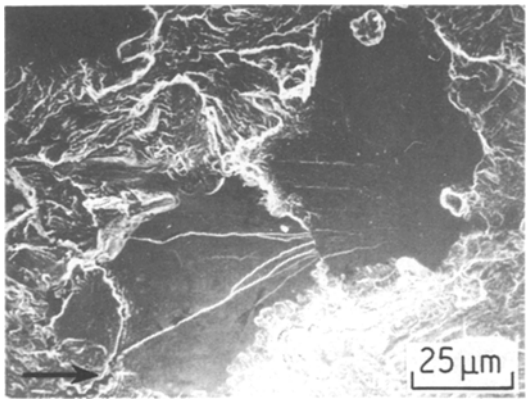

Figure 10 The fracture appearance at $\Delta K = 23$ MPa m$^{1/2}$. The arrow indicates the direction of microscopic crack growth of R0, $\eta = 3.9$.

TABLE IV Cyclic plastic zone size for each material

ΔK (MPa $m^{1/2}$)	Cyclic plastic zone size (μm) for: R0	R2	R4	R6
17	51	99	143	298
20	71	138	200	415
22	95	184	266	553

plastic constraint by the second phase; this is not mentioned in Suzuki and McEvily's paper [7].

4. Conclusions

(1) When the mechanism of fatigue crack propagation involves static modes with remarkable continuous cleavage cracking, the crack growth rate, da/dN, does not depend on stress intensity, ΔK.

(2) On the other hand, when the crack propagates mainly by striation, slipping at the advancing crack trip, crack propagation, da/dN, does depend on stress intensity, ΔK.

(3) On decreasing the strength ratio, crack propagation becomes independent of mean stress.

Acknowledgement

The support of Professsor S. Yoshida of the University of Tokyo in the carrying out of this study is appreciated.

References

1. P. C. PARIS, ASME paper, 62-MET-3 (1962).
2. P. C. PARIS and F. ERDOGAN, *Trans. ASME Ser. D.* **85** (1963) 528.
3. Y. TOMODA, G. KUROKI and I. TAMURA, *J. Iron Steel Inst. Japan* **61** (1975) 107.
4. H. W. HAYDEN and S. FLOREEN, *Met. Trans.* **1** (1970) 1955.
5. R. O. RITCHIE and J. F. KNOTT, *Acta Metall.* **21** (1973) 639.
6. C. E. RICHARDS and T. C. LINDLEY, *Eng. Fract. Mech.* **4** (1972) 951.
7. H. SUZUKI and A. J. MCEVILY, *Metall. Trans. A* **10A** (1979) 475.
8. T. ISHIHARA, *J. Jpn. Soc. Mech. Eng.* **46-410** (1980) 1026.
9. T. W. CROOKER, D. F. HASSON and G. R. YODER, *ASTM STP* **600** (1976) 209.
10. H. TADA, T. PARIS and G. IRWIN, "Stress Intensity Factor Handbook" (DEL Research Corporation, Pennsylvania, 1973) Chap. 2, p. 10.
11. T. ISHIHARA, *SAMPE Q.* (1982) to be published.
12. J. R. RICE, *ASTM STP* **415** (1967) 247.

Received 22 March
and accepted 27 May 1982